



The mechanical stimulation of cells in 3D culture within a self-assembling peptide hydrogel

Yusuke Nagai^{a,b}, Hidenori Yokoi^b, Keiko Kaihara^a, Keiji Naruse^{a,*}

^a Cardiovascular Physiology, Okayama University Graduate School of Medicine, Dentistry and Pharmaceutical Sciences, Japan

^b Menicon Co., Ltd., Japan

ARTICLE INFO

Article history:

Received 24 August 2011

Accepted 17 October 2011

Available online 5 November 2011

Keywords:

Cell proliferation

Self-assembly

Hydrogel

Scaffold

Mechanical strain

ABSTRACT

The aim of this present study was to provide a scaffold as a tool for the investigation of the effect of mechanical stimulation on three-dimensionally cultured cells. For this purpose, we developed an artificial self-assembling peptide (SPG-178) hydrogel scaffold. The structural properties of the SPG-178 peptide were confirmed by attenuated total reflection-Fourier transform infrared spectroscopy (ATR-FTIR) and transmission electron microscopy (TEM). The mechanical properties of the SPG-178 hydrogel were studied using rheology measurements. The SPG-178 peptide was able to form a stable, transparent hydrogel in a neutral pH environment. In the SPG-178 hydrogel, mouse skeletal muscle cells proliferated successfully (increased by 12.4 ± 1.5 times during 8 days of incubation; mean \pm SEM). When the scaffold was statically stretched, a rapid phosphorylation of ERK was observed (increased by 2.8 ± 0.2 times; mean \pm SEM). These results demonstrated that the developed self-assembling peptide gel is non-cytotoxic and is a suitable tool for the investigation of the effect of mechanical stimulation on three-dimensional cell culture.

© 2011 Elsevier Ltd. Open access under [CC BY-NC-ND license](http://creativecommons.org/licenses/by-nc-nd/3.0/).

1. Introduction

The goal of tissue engineering is to restore diseased or damaged tissue by delivering functional cells, scaffolds, and signal molecules such as growth factors to the affected area. The scaffolds should permit the release of the signal molecules and the ingress of nutrients and oxygen to keep the implanted cells alive. Furthermore, to elicit the implanted cell functions, the scaffolds should transmit several mechanical stimulations. The effects of mechanical stimulation have been proven in several cell culture systems, e.g., cardiomyocytes [1,2], chondrocytes [3,4], and others [5–7]. Animal-derived materials such as collagen and Engelbreth-Holm-Swarm (EHS) gels are widely used as scaffolds for tissue engineering because of their general compatibility with living tissues [8]. However, those scaffolds often contain growth factors, which may interfere with the estimation of the effects of the mechanical stimulation [9,10]. Furthermore, such animal-derived materials can cause allergic reactions [11,12] and carry dangerous pathogens including prions that cause a variety of neurodegenerative diseases in humans and animals. Evidence for the transmission of bovine spongiform encephalopathy prions to humans has been reported

[13]. Other viruses might also be carried as pathogens in animal-derived scaffolds. Thus, there is a need for alternative sources of animal-derived scaffolds.

Self-assembling peptides are one of the candidate materials to solve these problems. The complete sequence of a self-assembling peptide was originally found in a region of alternating hydrophobic and hydrophilic residues in zuotin [14], which is characterized by a stable β -sheet structure that undergoes self-assembly into nanofibers. The nanofibers form interwoven matrices that further form a hydrogel scaffold [15,16]. These hydrogel systems are well characterized and have already been employed in a variety of tissue engineering studies [17–20], drug delivery systems [21,22], and hemostatic applications [23]. Self-assembling peptides are a 100% chemically synthesized material. Therefore, the use of self-assembling peptide hydrogels can minimize the risk of biological contamination and the influence from the undefined factors in EHS gels.

However, a typical self-assembling peptide gel, RADA16 (RADARADARADA; R = arginine, A = alanine, and D = aspartic acid) gel, has a very low pH (approximately 3–4), thereby retaining the potential to harm inner cells and host tissues. In one particular case, a gel required one week to gradually change its pH from acidic to neutral by a solvent substitution [24]. In addition, an important drawback is that the RADA16 hydrogel structure is unstable under neutral conditions. After the neutralization procedure, the hydrogel

* Corresponding author.

E-mail address: knaruse@md.okayama-u.ac.jp (K. Naruse).

tends to break under mechanical stress [25]. Furthermore, once the hydrogel is stirred, the electrostatic interactions between the protonated arginine (+) and the deprotonated aspartic acid (–) within the RADA16 peptide strongly occur and yield a precipitate [26].

The aim of this study was to provide a scaffold as a tool for the investigation of the effect of mechanical stimulation on three-dimensionally cultured cells without any interference from undefined factors such as the growth factors in animal-derived scaffolds. For this purpose, we developed a self-assembling peptide, SPG-178 (Self-assembling Peptide Gel, amino acid sequence #178; $[\text{CH}_3\text{CONH}]\text{-RLDLRLALRLDLR}\text{-[CONH}_2\text{]}$; R = arginine, L = leucine, D = aspartic acid, and A = alanine; Fig. 1). It is well known that a protein reaches its minimum solubility at its isoelectric point, where the protein has a zero net charge. This property of proteins is closely related to the instability of the hydrogel formed by the RADA16 peptide, whose isoelectric point is 6.1 [26]. Therefore, the isoelectric point of the SPG-178 peptide was designed to be 11.5 by employing four cationic arginine and two anionic aspartic acid residues. Furthermore, leucine residues were employed to increase the hydrophobic interaction among the SPG-178 peptides, which was the main driving force of the self-assembly, and stabilize the hydrogel formation.

We report here on the biocompatibility of a developed self-assembling peptide hydrogel and its ability to transmit mechanical stimulation. Murine C2C12 myoblast cells were used for all of the cell culture experiments because they are known to be acutely responsive to mechanical stimulation.

2. Materials and methods

2.1. Self-assembling peptide SPG-178

The self-assembling peptide SPG-178, $[\text{CH}_3\text{CONH}]\text{-RLDLRLALRLDLR}\text{-[CONH}_2\text{]}$, was synthesized by a solid-phase method using standard Fmoc strategy (see Supplementary Data and Fig. S1). The peptide powder was dissolved in a 10% (w/v) sucrose solution. Then the peptide solution was sterilized by filtration through a 0.22 μm filter. The pH of the peptide solution was adjusted to approximately pH = 6.5 by adding aliquots of a 0.5% (w/v) sodium hydrogen carbonate solution. The final concentration of the peptide in the solution was 2.4 mM (0.4% w/v).

2.2. CPK model of SPG-178 peptide

The molecular models of the anti-parallel β -sheet structure and the fiber formation of the SPG-178 peptide were produced using Facio, a 3D-graphics program, and employing Tinker with a charm 22 force field parameter (<http://www1.bbiq.jp/zzfelis/Facio.html> and <http://dasher.wustl.edu/tinker/>) [27,28]. The dimension of the peptide monomer was calculated using Swiss-PdbViewer (<http://www.expasy.org/spdbv/>) [29] (Fig. 1A).

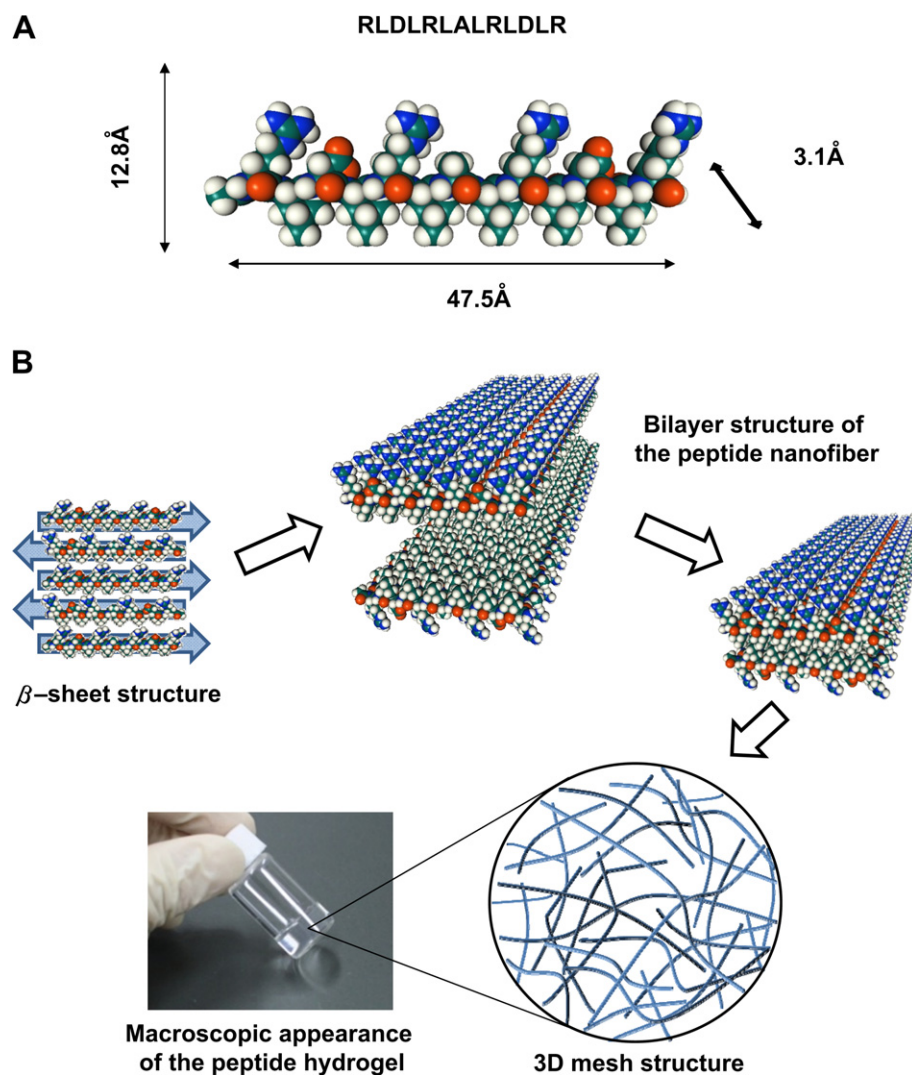


Fig. 1. The self-assembling peptide SPG-178 hydrogel scaffold. (A) A molecular model of SPG-178, the dimensions of which are $47.5 \times 12.8 \times 3.1$ Å. For the representation, Facio was used: cyan, carbon; red, oxygen; blue, nitrogen; white, hydrogen. (B) A schematic diagram of the formation of the hydrogel from the peptide monomer. (For interpretation of the references to colour in this figure legend, the reader is referred to the web version of this article.)

2.3. Gel stretch chamber

In this study, a gel stretch chamber was employed for the three-dimensional cell culture and the tension experiments. The gel stretch chamber was constructed by attaching a piece of silicone foam sheet (SPP-2.0S, AS ONE, Osaka, Japan) that had been manually cut to a size of approximately 20 mm × 4.5 mm × 2 mm (length × width × thickness), with a rectangular hole of approximately 18 mm × 1.5 mm (length × width) for holding the peptide gel, to the inner wall of a commercially available stretch chamber (STB-CH-04, STREX, Osaka, Japan). Silicone resin (TSE3032, GE Toshiba Silicones, Tokyo, Japan) was used as a glue. The silicone foam sheet was located approximately 2 mm above the bottom of the chamber to allow the cell culture medium to contact the bottom of the hydrogel. A hydrophilic surface treatment, which consisted of high power plasma sterilization (PDC-32G, Harrick Scientific Products Inc., NY, USA) for 10 min, was performed to increase the hydrophilicity of the silicone foam sheet surface before its use.

2.4. Attenuated total reflection-Fourier transform infrared spectroscopy (ATR-FTIR)

The sample for the ATR-FTIR was prepared by dissolving SPG-178 peptide powder in a deuterated aqueous solution at a final concentration of 1% (w/v). The pH of the sample was adjusted to approximately pH = 6.5 by adding aliquots of a 0.5% (w/v) sodium hydrogen carbonate solution. The sample formed a hydrogel at this condition (1% [w/v] at pH = 6.5), which indicated the presence of nanofibers and the three-dimensional network structure formation of the SPG-178 peptide. The spectrum was recorded on a Perkin-Elmer Spectrum One spectrometer equipped (Perkin-Elmer, Norwalk, CT, USA) with a Horizontal ATR (HATR) Sampling Accessory and a trough plate, which was comprised of a ZnSe crystal with a 45° angle of incidence. One milliliter of the hydrogel was spread directly onto the surface of the trough plate. The spectrum was recorded at room temperature from 4000 cm⁻¹ to 650 cm⁻¹, and 32 scans were collected with a spectral resolution of 4 cm⁻¹. A deuterated water spectrum was used as background and was subtracted from the sample spectrum.

2.5. Transmission electron microscopy (TEM)

Dulbecco's modified Eagles medium (DMEM; WAKO, Osaka, Japan) was mixed with the peptide solution described in Section 2.1 at a volume ratio of 1:2. The mixture formed a hydrogel due to the increased salt concentration [14,15,30] even though the peptide concentration was lowered from 2.4 mM to 1.6 mM. The final concentration of the SPG-178 peptide in the hydrogel was 1.6 mM. A 60 µl aliquot of the hydrogel was added to the rectangular hole in the silicone foam sheet in the gel stretch chamber. The chamber was filled with 3 ml of DMEM that was supplemented with 10% (v/v) fetal bovine serum (FBS) and incubated in 5% CO₂ at 37 °C for 8 days. After the incubation, the DMEM supplemented with 10% (v/v) FBS was removed, and the hydrogel was fixed in a 0.1 M phosphate buffer containing 2% (v/v) glutaraldehyde and 2% (v/v) paraformaldehyde at 4 °C over night and postfixed in 2% (w/v) osmium tetroxide for 2 h at room temperature. The SPG-178 hydrogel was dehydrated using graded concentrations of ethanol. After dehydration, the hydrogel was embedded in Spurr resin (Polysciences, Warrington, PA, USA). Ultrathin sections (60–90 nm) were cut with a Leica EM UC6 ultramicrotome (Leica, Vienna, Austria) and stained with uranyl acetate and lead citrate. Visualization was performed using a Hitachi 7650 electron microscope (Hitachi, Tokyo, Japan), which was operated at 80 kV.

2.6. Rheology measurement

The SPG-178 hydrogel, which contained 1.6 mM of the SPG-178 peptide was prepared as described in Section 2.5. A 40 µl aliquot of the hydrogel was placed on the plate of a rheometer (AR1000, TA Instruments, New Castle, DE, USA). A 20-mm-diameter, 1° aluminum cone with truncation at 24 µm was lowered so that the tip was 24 µm above the plate. A solvent trap was used to maintain a water-saturated atmosphere to prevent the evaporation of solvent during the measurement. The SPG-178 hydrogel was tested over a range of frequencies from 10 to 0.1 rad/s at 1.0 µNm oscillatory torque to measure the storage modulus (G' , the elastic response) and the loss modulus (G'' , the viscous response) at 37 °C. As controls, a 2.4 mM SPG-178 peptide solution and DMEM were tested in the same manner.

2.7. Three-dimensional cell culture

Murine C2C12 myoblasts (ECACC: 91031101) were obtained from the European Collection of Cell Cultures (DS Pharma Biomedical, Osaka, Japan). The C2C12 cells were cultured on a Petri dish and grown until 50% confluence in DMEM supplemented with 10% (v/v) FBS in 5% CO₂ at 37 °C. To start the three-dimensional cell culture, the cells were trypsinized and suspended in DMEM and then mixed with a 2.4 mM SPG-178 peptide solution at a volume ratio of 1:2. The final concentration of the cells and the peptide in the hydrogel were 2 × 10⁶ cells/ml and 1.6 mM, respectively. A 60 µl aliquot of the hydrogel was added in the rectangular hole of the

silicone foam sheet in the gel stretch chamber. For the cell proliferation assay, the same amount of the hydrogel was added to a 1.5 ml tube and stored at -80 °C (day 0 control). The chamber was filled with 3 ml of DMEM that was supplemented with 10% FBS and incubated in 5% CO₂ at 37 °C. The medium was replaced with 3 ml of fresh medium once every 2–3 days.

2.8. Live and dead assay

C2C12 cells were cultured in the SPG-178 hydrogel as described in Section 2.7. On the 8th day of incubation, the medium was changed to DMEM. Calcein (calcein-AM, Dojindo, Kumamoto, Japan) and 4,6-diamidino-2-phenylindole, dihydrochloride (DAPI, Dojindo) were added to the gel stretch chamber at a final concentration of 10 µM to stain the nuclei of live and dead or injured cells. After 30 min of incubation in 5% CO₂ at 37 °C, the stained cells that were located approximately 500 µm above the bottom of the hydrogel were observed on a confocal laser scanning microscopy system (ex/em = 405/460 nm for DAPI and 488/515 nm for calcein, FV-1000, Olympus, Tokyo, Japan).

2.9. Cell proliferation assay

C2C12 cell proliferation in the SPG-178 hydrogel was measured with a CyQUANT Cell Proliferation Assay Kit (C7026, Molecular Probes, Eugene, OR, USA) with small modifications to the manufacturer's protocol. The hydrogels described in Section 2.7 were transferred from the gel stretch chamber to a 1.5 ml tube after 2, 4, 6, and 8 days of incubation and were stored at -80 °C for at least one hour before the assay. After collecting and storing all of the samples, the hydrogels, including the day 0 control described in Section 2.7, were thawed and dispersed into 940 µl of Cell-Lysis Buffer (1X component B). Ten microliters of each dispersed gel solution were transferred to a well of a 96-well plate. Two hundred microliters of CyQUANT GR dye solution (a mixture of 1X component A and 1X component B) were added to each well and measured on a spectrofluorometer with the FLUO star OPTIMA software. The number of cells in the gel mixture was extrapolated from a standard curve that was generated with known amount of C2C12 cells over a range of 6 × 10² cells – 2.4 × 10⁴ cells per well.

2.10. Stretching cells in the SPG-178 hydrogel

C2C12 cells were cultured in the peptide gel as described in Section 2.7, with the exception of changing the SPG-178 hydrogel volume from 60 µl to 90 µl. The volume increase allowed for the deep intrusion of the hydrogel into the cavities of the silicone foam, which resulted in the prevention of the detachment of the hydrogel during the stretch. The gel stretch chamber was placed into a hand-control stretch device (STB-10, STREX). On the 5th day of incubation, the cells in the hydrogel were stained by adding calcein-AM in the chamber at a final concentration of 10 µM. After 30 min of incubation, the chamber was statically stretched by 20%. The stained cells that were located approximately 500 µm above the bottom of the hydrogel were observed on the confocal laser scanning microscopy system FV-1000 before and after the stretch.

2.11. Static stretch for ERK activation

C2C12 cells were cultured in the peptide gel as described in Section 2.10. On the 8th day of incubation, the medium was changed from DMEM that was supplemented with 10% FBS to a low serum differentiation medium (DMEM supplemented with 2% [v/v] horse serum). After an additional 2 days of incubation, the gel stretch chamber was statically stretched by 10% for 5 min in 5% CO₂ at 37 °C (Stretched sample; ST). Parallel sets of non-stretched C2C12 cells that were cultured in the SPG-178 hydrogels in the gel stretch chamber were used as a control (Non-stretch control; NST). MEK1 inhibitor (PD98059, Cell Signaling Technology, Beverly, MA, USA) that was dissolved in DMSO was added to the gel stretch chamber as necessary to achieve a final concentration of 50 µM one hour before the stretch (Stretched sample with PD98059; STP). The control samples for the inhibitor were treated with the same volume of vehicle DMSO (Stretched sample with DMSO; STD). After the completion of the stretch, the SPG-178 hydrogel was collected for Western Blotting.

2.12. Western blotting

The SPG-178 hydrogels were transferred to a 1.5 ml tube that contained 1 ml of ice-cold TBS with protease and phosphatase inhibitors (1% [v/v], 78440, Thermo Fisher Scientific, Rockford, IL, USA) to remove any excess medium in and on the gel. The tube was centrifuged at 1200 × g (3550 rpm) for 5 min at 4 °C, the supernatant was discarded, and 100 µl of RIPA lysis buffer (Thermo Fisher Scientific, Rockford, IL, USA) with the protease and phosphatase inhibitors were added. The cell lysate was sonicated for a total of 25 s with a sonicator (BRANSON Digital Sonifier II, BRANSON, Danbury, CT, USA) to break down the gel fiber structure and was cleared at 21,500 × g (15,000 rpm) for 45 min at 4 °C. The supernatants were transferred into new tubes and quantified using the BCA protein assay kit (Pierce, Rockford, IL, USA). Approximately 25 µg of protein were loaded in a 10% SDS polyacrylamide gel

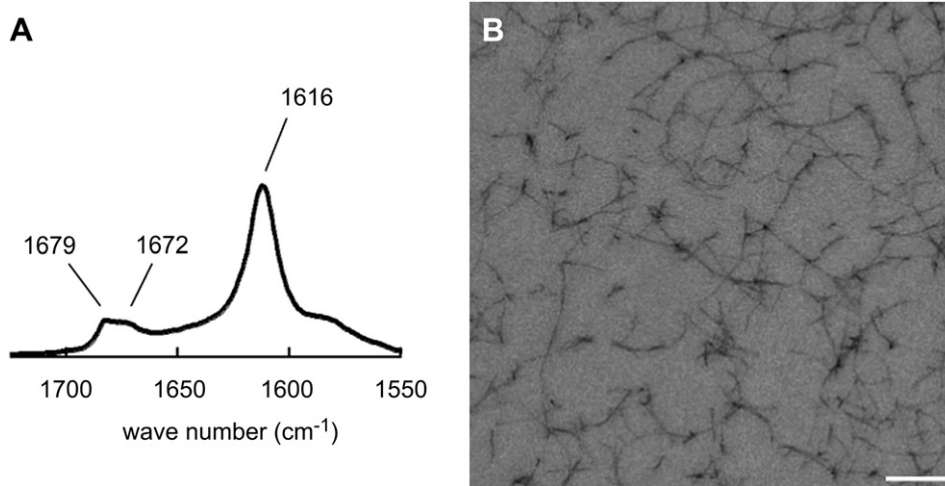


Fig. 2. The structural properties of SPG-178. (A) ATR-FTIR spectra of the SPG-178 peptide solution. (B) A TEM image of the peptide nanofibers in the hydrogel. The scale bar is 200 nm.

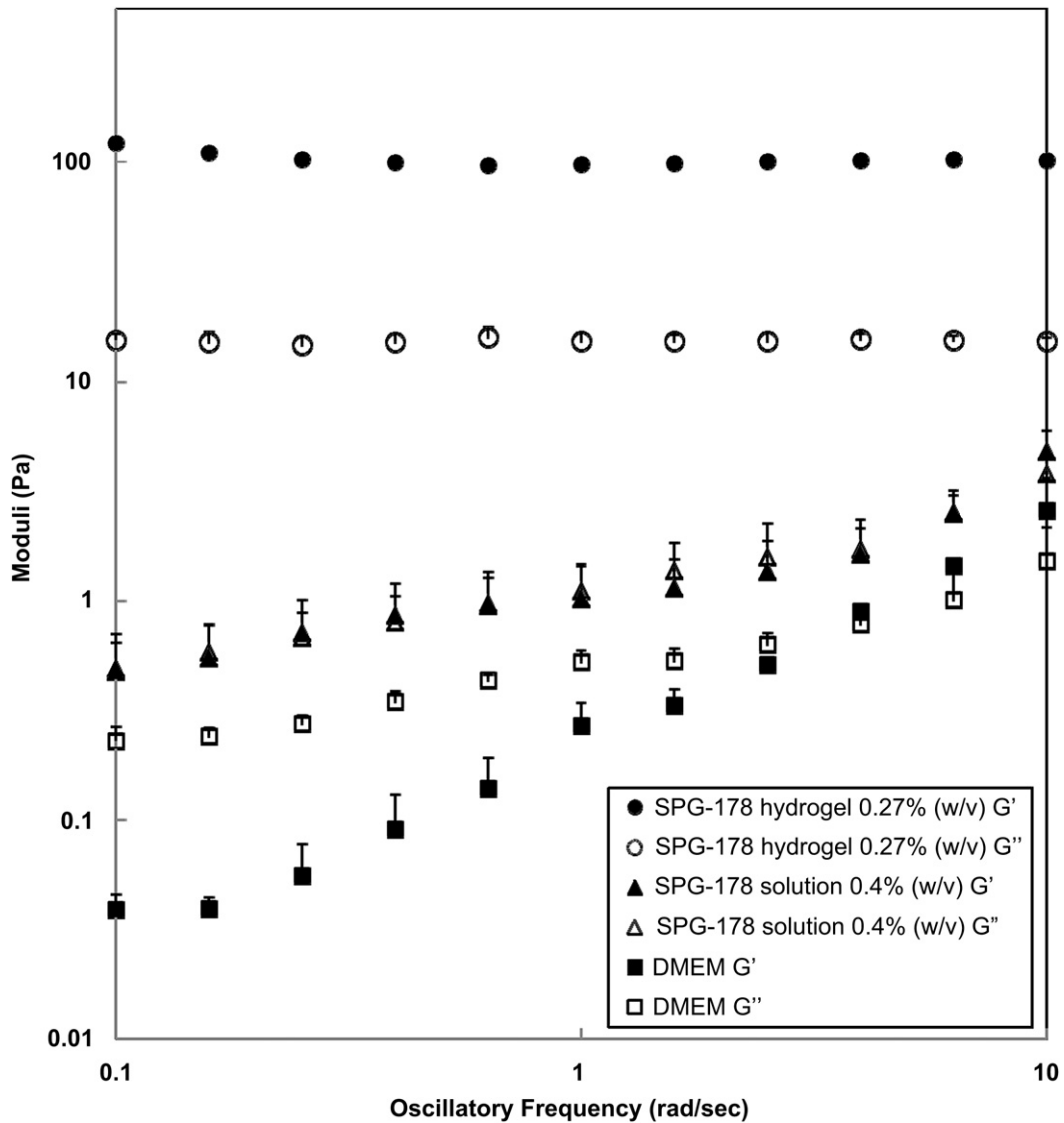


Fig. 3. The mechanical properties of the SPG-178 hydrogel. (●) SPG-178 hydrogel 0.27% (w/v) G', (○) SPG-178 hydrogel 0.27% (w/v) G'', (▲) SPG-178 solution 0.4% (w/v) G', (△) SPG-178 solution 0.4% (w/v) G'', (■) DMEM G', (□) DMEM G''. Bars represent the mean ± SEM. (n = 3).

(SDS–PAGE) and transferred to an Immobilon-P transfer membrane (Millipore, Bedford, MA, USA). The membrane was blocked in 10% Blocking One (Nacalai Tesque, Kyoto, Japan) in TBS and incubated with primary antibodies: anti-ERK (4695, 1:1,000, Cell Signaling Technology), and anti-Phosphorylated ERK (Thr202/Tyr204; 4370, 1:1,000, Cell Signaling Technology). The blots were developed by chemiluminescence using LumiGLO (Cell Signaling Technology) to quantify the relative intensities (RI) and a tetramethylbenzidine (TMB) solution (EzWestBlue, Atto, Tokyo, Japan) to show a representative blot.

3. Results

3.1. ATR-FTIR

The existence of a β -sheet structure within the hydrogel was supported by ATR-FTIR spectroscopy (Fig. 2A). The spectra showed predominant peaks at 1616 cm^{-1} , which indicated the presence of aggregated β -sheets. The typical amide groups containing a β -sheet structure give rise to peaks ranging from 1620 cm^{-1} to 1640 cm^{-1} . The small peak at 1679 cm^{-1} suggested the presence of anti-parallel β -sheets in the nanofiber structure of the SPG-178 hydrogel. In contrast, there was no peak regarding helical character ($1640\text{--}1660\text{ cm}^{-1}$). Trace amounts of TFA accounted for the peak observed at 1672 cm^{-1} in the spectrum.

3.2. TEM

The TEM image from the ultrathin layer of the SPG-178 hydrogel showed the nanofibers and the network structure in the hydrogel (Fig. 2B). The diameter of the nanofibers was estimated to be less than 10 nm, which corresponds to the calculated length of the SPG-178 peptide monomer in β -sheet form (Fig. 1A). Partial mesh structures that were formed by the nanofibers were observed. The mesh size was variable, reaching up to 500 nm.

3.3. Mechanical properties of the SPG-178 hydrogel

Frequency sweep measurements of the SPG-178 hydrogel (1.6 mM) showed that the storage modulus (G' , the elastic response) and the loss modulus (G'' , the viscous response) values were relatively constant and that the G' values were much greater than zero. In addition, the G' values over the entire frequency range exceeded those of G'' . This result reflected the gel-like property of the SPG-178 hydrogel [26,30]. In contrast, the G' and G'' values obtained from the measurement with the DMEM sample, used as a representative example of a liquid, were low and decreased in an oscillatory manner. The result from the measurement with a 2.4 mM SPG-178 peptide solution was relatively similar to that of the DMEM sample and demonstrated a liquid-like property [26,30]. The G' and G'' values were very close at each oscillatory frequency (Fig. 3).

3.4. Live and dead, and cell proliferation assays

In the live and dead assay, the extended shapes of the C2C12 cells that were stained with calcein and a certain number of the nuclei stained with DAPI were observed in the SPG-178 hydrogel (Fig. 4A–C). Whereas the live/dead cell ratio of the observed area was lower than that of the surface area of the hydrogel (data not shown), the extended cells clearly showed that the hydrogel provided a suitable interface for the cells to adhere and survive. C2C12 cell proliferation in the SPG-178 peptide hydrogel scaffold was monitored by conducting DNA analysis for up to 8 days. As shown in Fig. 4D, the C2C12 cells proliferated gradually through 8 days of culture. Based on the measured DNA content, the estimated number of C2C12 cells in the hydrogel had increased by 12.4 ± 1.5 (mean \pm SEM, $n = 4$) times by the end of the incubation period.

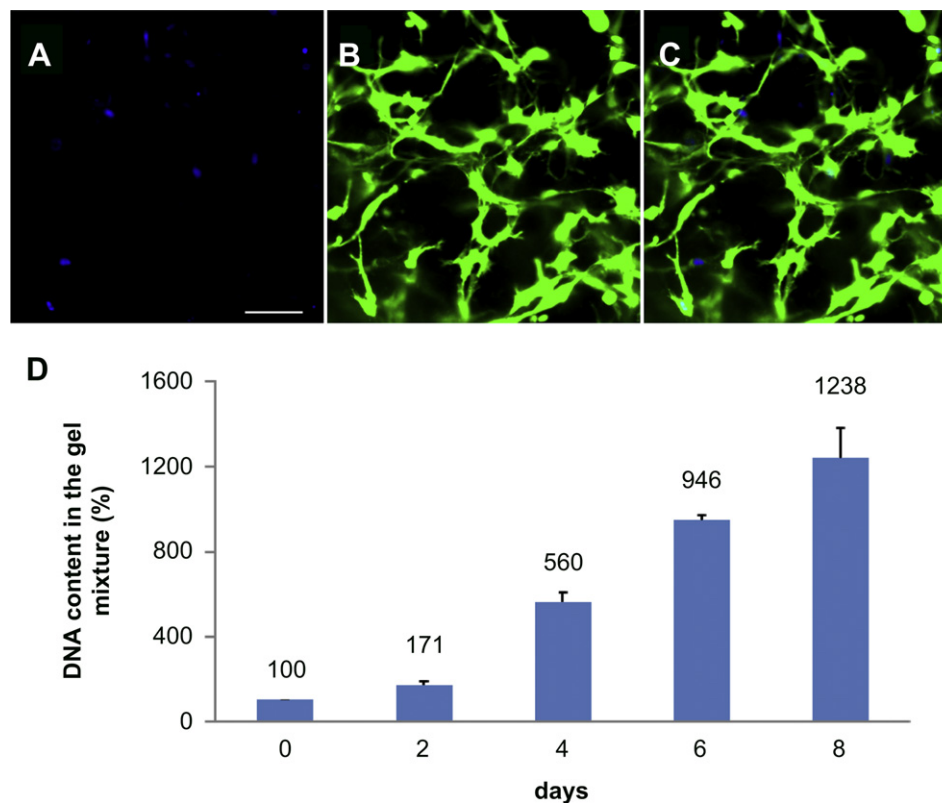


Fig. 4. Live and dead assay and cell proliferation assay. C2C12 cells in an SPG-178 hydrogel were stained with A) DAPI and B) calcein. The merged image is shown in (C). The proliferation of the C2C12 cells in the peptide gel was estimated by measuring DNA content (D). Scale bar shown in (A) is 50 μm . Bars represent mean \pm SEM. ($n = 4$).

3.5. Stretching cells in the SPG-178 hydrogel

The elongation of C2C12 cells in the SPG-178 hydrogel was observed as the gel stretch chamber was stretched by 20% with the hand-control stretch device STB-10 (Fig. 5). The distance between the asterisks was 260 μm before the stretch (Fig. 5A) and 310 μm after the stretch (Fig. 5B). The calculated ratio of the increased in distance was 19%, which corresponded to the stretch ratio of the gel stretch chamber. The successful cell stretch in the hydrogel indicated the deep intrusion of the SPG-178 hydrogel into the cavities of the silicone foam; therefore, the hydrogel was able to transmit the mechanical stress to the cells that were incorporated into the hydrogel. This result proved the usability of the stretch system for three-dimensionally cultured cells that consisted of the SPG-178 hydrogel, the gel stretch chamber, and the hand-control stretch device STB-10.

3.6. ERK phosphorylation by mechanical stimulation

Western blot analysis revealed that ERK in the three-dimensionally cultured C2C12 was activated by a static stretch (Fig. 6). The degree of the ERK phosphorylation was increased by

2.8 \pm 0.2 (mean \pm SEM, $n = 15$) times by the 5-min stretch (ST) compared to the untreated control basal value (NST: 1.0 \pm 0.1, mean \pm SEM, $n = 8$). The addition of 50 μM PD98059 completely inhibited the stretch-induced phosphorylation of ERK (STP), whereas the addition of DMSO, a solvent of PD98059, did not significantly affect the ERK phosphorylation (STD). The degree of the ERK phosphorylation was 0.6 \pm 0.1 (mean \pm SEM, $n = 8$) in STP and 2.3 \pm 0.3 (mean \pm SEM, $n = 7$) in STD. The blocking effect of the PD98059 emphasized the effect of the brief stretch on the ERK phosphorylation in three-dimensionally cultured cells. No change in the total ERK protein concentration was observed in any sample.

4. Discussion

In previous studies, self-assembling peptides with a total net charge of +2 have been reported to successfully form a hydrogel at pH = 7.4 [26,31]. The SPG-178 peptide solution (2.4 mM) is transparent and able to form a stable hydrogel at neutral pH when it is triggered by an increase in salt concentration (Fig. 1B). The stability of the peptide solution/hydrogel at neutral pH contributes to the biocompatibility of the scaffold and provides an additional benefit for the sterilization procedure. In fact, the SPG-178 solution at neutral pH can be sterilized with an autoclave. Insignificant degradation of the SPG-178 peptide was detected with MALDI-TOFF MASS (see Fig. S1 and S2), and no change in the gelation behavior was caused by autoclaving. In contrast, collagen scaffolds require relatively complicated procedures and expensive equipment, such as ethylene oxide gas treatment and γ -irradiation due to thermal denaturation [32]. The decomposition of the conventional self-assembling peptide RADA16 provided with low pH (Puramatrix, Becton Dickinson, CA, USA) by autoclaving was confirmed by MALDI-TOFF MASS (see Fig. S3 and S4).

In the structural studies, the ATR-FTIR spectra shown in Fig. 2A indicated the presence of considerable anti-parallel β -sheet content with no or negligible helical component in the SPG-178 hydrogel, as has been observed for conventional self-assembling peptides [16]. The TEM image from the ultrathin layer of the SPG-178 hydrogel demonstrated the nanofiber structure of the self-assembled peptide with a diameter of less than 10 nm. Taken together, the gelation process of the SPG-178 peptide was confirmed to correspond with the molecular models shown in Fig. 1. The partial mesh structure that was formed by the peptide nanofibers was observed in the TEM image. Some of the other nanofibers that seemed too short to form the mesh structure were considered to have been cut in the procedure for preparing the ultrathin layer. The average length of the nanofiber was difficult to be estimated from the image for the same reason. However, the mesh size (approximately 500 nm) of the SPG-178 hydrogel was considered to be much smaller than the size of the cells (approximately 10 μm). Since, the SPG-178 peptide nanofibers are not chemically cross-linked, the mesh structure of the hydrogel can easily change. Thus, the pore size of the hydrogel is considered to widen and be rebuilt as cells in the hydrogel infiltrate or ingrow.

The gel-like property of the SPG-178 hydrogel was demonstrated with the rheology measurement. Both the storage modulus, G' , and the loss modulus, G'' , of the hydrogel were relatively low compared to other self-assembling peptides [33]. This can be explained by the lower concentration of the SPG-178 in the hydrogel (0.27% [w/v]) compared to the other approximately 2% (w/v) hydrogels. The low mechanical strength of the SPG-178 hydrogel contributes to the homogeneous distribution of the cells in the mixing process at the beginning of the cell culture. Next, the further increase in the salt concentration during the immersion of the SPG-178 hydrogel into the cell culture medium will enhance the gelation to increase the mechanical strength of the hydrogel.

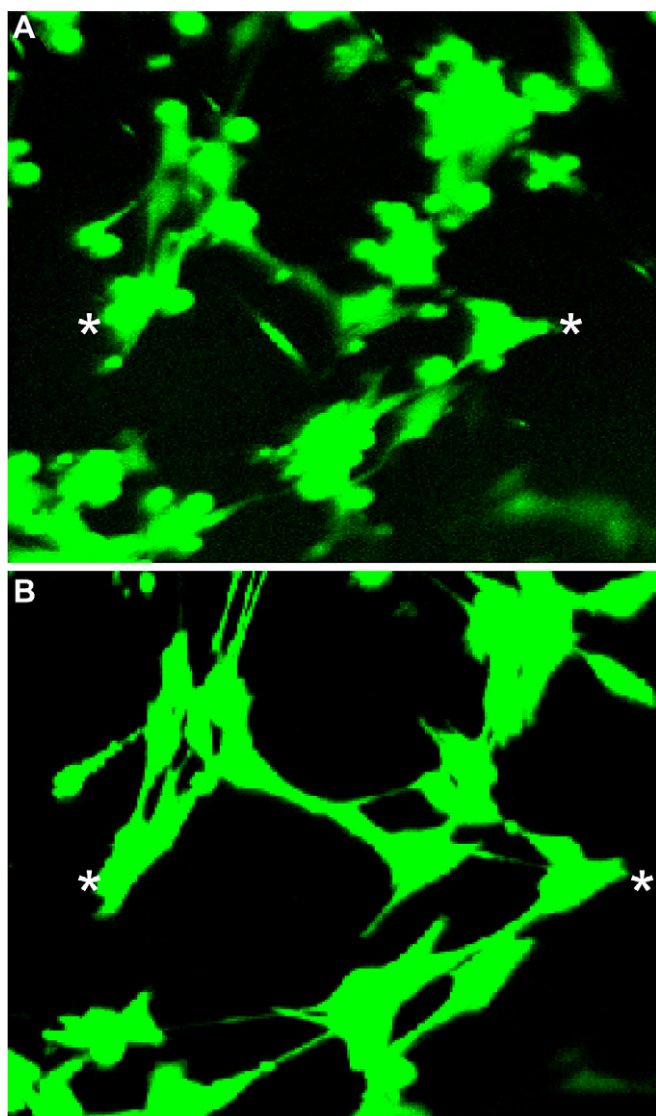


Fig. 5. C2C12 cells in the peptide gel stained with calcein-AM (A) before and (B) after the stretch (20%) in the stretch chamber. The intercellular distance between the asterisks was 260 μm before the stretch and 310 μm after the stretch.

In the live and dead assay, the extended shapes of the C2C12 cells were observed in the SPG-178 hydrogel, which indicated tight cell adhesion onto the peptide nanofiber. In addition, the DNA content measurement revealed that the three-dimensionally cultured C2C12 cells proliferated successfully during the incubation. These results indicate that the SPG-178 hydrogel is suitable as a scaffold. According to the mesh size (approximately 500 nm) of the SPG-178 observed by TEM, the cells must be suspended in the three-dimensional nanofiber network of the SPG-178 hydrogel. The charged amino acid residues within the peptide nanofiber, especially the positively charged arginine residues, are considered to support cell adhesion at the beginning of the culture [34,35]. The serum proteins in the cell culture medium may also attach to the peptide nanofiber and help the cell adhesion [36]. Furthermore, there are studies introducing a cell adhesion motif such as RGD in self-assembling peptide hydrogels to improve cell adhesion and survival ratios [37,38]. These techniques might also be useful for the SPG-178 hydrogel. In other studies using rat skeletal muscle cell (L6) and human chondrosarcoma cells (OUMS-27), accumulated type-I collagen and aggrecan in the SPG-178 hydrogel were observed, respectively (unpublished data). These secreted and accumulated ECM components in the hydrogel are expected to contribute to the cell proliferation and migration. Further research is needed to understand the detailed mechanism of cell adhesion, extension, and migration in SPG-178 hydrogels.

The confocal microscope observations showed the elongation of the cells and the increased distance between the cells as the peptide gel was stretched. These results proved that the peptide gel scaffold was “stretchable” and capable of transmitting the mechanical stimulation to the inner cells. The plasma-treated hydrophilic surface of the silicone foam sheet and the low mechanical strength (low viscosity) of the SPG-178 hydrogel facilitated the deep infiltration of the hydrogel into the cavities of the silicone foam. Thus, the expanded area of contact between the silicone foam sheet and the hydrogel produced a friction force that was great enough to stretch the hydrogel without slipping.

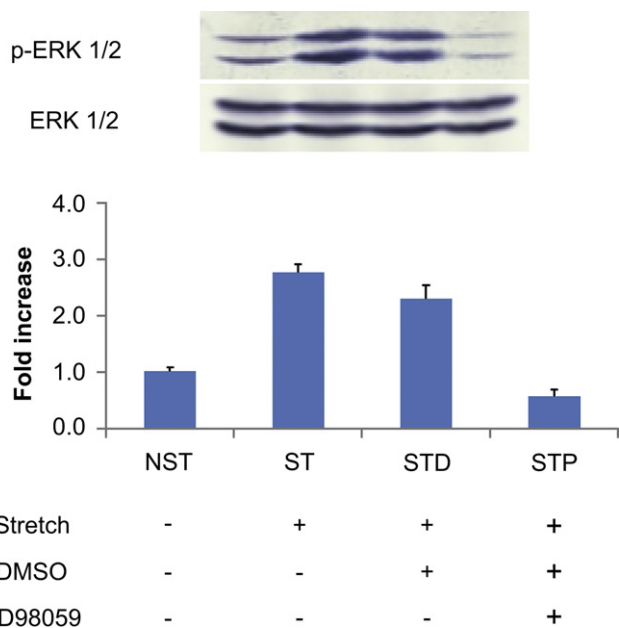


Fig. 6. Western Blot analysis. A representative blot of phosphorylated ERK (p-ERK1/2) and total ERK (ERK1/2) showed an increased intensity in labeling of phosphospecific ERK antibody following the stretch, and the effect of the MEK inhibitor PD98059. Bars represent mean \pm SEM ($n = 8$ (NST), 15 (ST), 7 (STD), 8(STP)).

Consequently, the stretch system that consisted of the SPG-178 hydrogel, the gel stretch chamber, and the hand-control stretching device STB-10 was confirmed to be usable for the stretching of three-dimensionally cultured cells.

Stretch-induced ERK phosphorylation have been previously shown in many papers including studies in the two-dimensional cell culture of C2C12 cells [39,40], fibroblast cells [41–43], human keratinocytes [44], and whole rat skeletal muscle stretching [45]. In these studies, the peak time of the ERK phosphorylation varied because of the different cell cultures and stretch systems. However, generally, the ERK phosphorylation started in the early stage of the stretch induction in these studies. In our study, the ERK in the C2C12 cells were also activated quickly by stretching in the SPG-178 hydrogel. The transmission of the mechanical stimulation was supported by the friction force between the gel stretch chamber and the SPG-178 hydrogel and the cell adhesion to the peptide nanofiber network. The gel stretch chamber can be incorporated in an automatic stretch system suitable for cyclical stretching or a long-term stretching experiment to investigate the cellular response to mechanical stress in three-dimensional cell culture.

5. Conclusions

Mechanical stimulation is now widely incorporated into three-dimensional cell culture systems for tissue engineering. We studied the biocompatibility and the ability to transmit mechanical stimulation of a self-assembling peptide hydrogel. The self-assembling peptide SPG-178 was 100% chemically synthesized and was confirmed to form an anti-parallel β -sheet structure in aqueous solution. The peptide self-assembled to form a nanofiber with a diameter of less than 10 nm, which further formed a hydrogel. The results of the three-dimensional cell culture clarified that the developed self-assembling peptide gel was non-cytotoxic. Western Blot analysis demonstrated the rapid phosphorylation of ERK induced by the static stretching of the hydrogel. These results indicated that the self-assembling peptide hydrogel was a suitable tool for the investigation of the effect of mechanical stress on three-dimensional cell culture. Additional studies are needed for a better understanding of the contribution from the secreted ECM component.

Acknowledgments

We thank Ms. Masumi Furutani for her efficient technical support in obtaining the TEM images and Dr. Ken Takahashi for the helpful discussions on the experimental details. We are indebted to Dr. Yasuyuki Ishida at Chubu University for generously allowing us use of a MALDI-TOF mass spectrometer. This work was partially supported by Grant-in-Aid for Scientific Research of Priority Areas, 17076006 provided by the Ministry of Education, Culture, Sports, Sciences, and Technology of Japan (to K.N.), and Challenging Exploratory Research, 23650264 provided by the Japanese Society for the Promotion of Science (to K.N.). Y.N. and H.Y. were supported by Menicon Co., Ltd., Japan.

Appendix. Supplementary data

Supplementary data related to this article can be found online at doi:10.1016/j.biomaterials.2011.10.049.

References

- [1] Zimmermann WH, Melnychenko I, Wasmeier G, Didié M, Naito H, Nixdorff U, et al. Engineered heart tissue grafts improve systolic and diastolic function in infarcted rat hearts. *Nat Med* 2006;12:452–8.

- [2] Akhyari P, Fedak PWM, Weisel RD, Lee TYJ, Verma S, Mickle DAG, et al. Mechanical stretch regimen enhances the formation of bioengineered autologous cardiac muscle grafts. *Circulation* 2002;106:1-137–42.
- [3] Hirano Y, Ishiguro N, Sokabe M, Takigawa M, Naruse K. Effects of tensile and compressive strains on response of a chondrocytic cell line embedded in type I collagen gel. *J Biotechnol* 2008;133:245–52.
- [4] Hunter CJ, Mouw JK, Levenston ME. Dynamic compression of chondrocyte-seeded fibrin gels: effects on matrix accumulation and mechanical stiffness. *Osteoarthritis Cartilage* 2004;12:117–30.
- [5] Powell CA, Smiley BL, Mills J, Vandenberg HH. Mechanical stimulation improves tissue-engineered human skeletal muscle. *Am J Physiol Cell Physiol* 2002;283:C1557–65.
- [6] Androjna C, Spragg RK, Derwin KA. Mechanical conditioning of cell-seeded small intestine submucosa: a potential tissue-engineering strategy for tendon repair. *Tissue Eng* 2007;13:233–43.
- [7] Ignatius A, Blessing H, Liedert A, Schmidt C, Neidlinger-Wilke C, Kaspar D, et al. Tissue engineering of bone: effects of mechanical strain on osteoblastic cells in type I collagen matrices. *Biomaterials* 2005;26:311–8.
- [8] Lee CH, Singla A, Lee Y. Biomedical applications of collagen. *Int J Pharm* 2001; 221:1–22.
- [9] Vukicevic S, Kleinman HK, Luyten FP, Roberts AB, Roche NS, Reddi AH. Identification of multiple active growth factors in basement membrane matrigel suggests caution in interpretation of cellular activity related to extracellular matrix components. *Exp Cell Res* 1992;202:1–8.
- [10] Vallier L, Alexander M, Pedersen RA. Activin/Nodal and FGF pathways cooperate to maintain pluripotency of human embryonic stem cells. *J Cell Sci* 2005; 118(19):4495–509.
- [11] Cooperman L, Michaeli D. The immunogenicity of injectable collagen. I. A 1-year prospective study. *J Am Acad Dermatol* 1984;10:638–46.
- [12] Lynn AK, Yannas IV, Bondfield W. Antigenicity and immunogenicity of collagen. *J Biomed Mater Res Part B Appl Biomater* 2004;71B(2):343–54.
- [13] Scott MR, Will R, Ironside J, Nguyen HOB, Tremblay P, DeArmond SJ, et al. Compelling transgenic evidence for transmission of bovine spongiform encephalopathy prions to humans. *Proc Natl Acad Sci USA* 1999;96: 15137–42.
- [14] Zhang S, Holmes TC, Lockshin C, Rich A. Spontaneous assembly of a self-complementary oligopeptide to form a stable macroscopic membrane. *Proc Natl Acad Sci USA* 1993;90:3334–8.
- [15] Zhang S, Holes TC, DiPersio CM, Hynes RO, Su X, Rich A. Self-complementary oligopeptide matrices support mammalian cell attachment. *Biomaterials* 1995;16:1385–93.
- [16] Yokoi H, Kinoshita T, Zhang S. Dynamic reassembly of peptide RADA16 nanofiber scaffold. *Proc Natl Acad Sci USA* 2005;102:8414–9.
- [17] Semino CE, Merok JR, Crane GG, Panagiotakos G, Zhang S. Functional differentiation of hepatocyte-like spheroid structures form putative liver progenitor cells in three-dimensional peptide scaffolds. *Differentiation* 2003;71: 262–70.
- [18] Genové E, Shen C, Zhang S, Semino CE. The effect of functionalized self-assembling peptide scaffolds on human aortic endothelial cell function. *Biomaterials* 2005;26:3341–51.
- [19] Davis ME, Motion JPM, Narmoneva DA, Takahashi T, Hakuno D, Kamm RD, et al. Injectable self-assembling peptide nanofibers create intramyocardial microenvironments for endothelial cells. *Circulation* 2005;111:442–50.
- [20] Holmes TC, De Lacalle S, Su X, Liu G, Rich A, Zhang S. Extensive neurite outgrowth and active synapse formation on self-assembling peptide scaffolds. *Proc Natl Acad Sci USA* 2000;97:6728–33.
- [21] Nagai Y, Unsworth LD, Koutsopoulos S, Zhang S. Slow release of molecules in self-assembling peptide nanofiber scaffold. *J Control Release* 2006;115:18–25.
- [22] Koutsopoulos S, Unsworth LD, Nagai Y, Zhang S. Controlled release of functional proteins through designer self-assembling peptide nanofiber hydrogel scaffold. *Proc Natl Acad Sci USA* 2008;106:4623–8.
- [23] Ellis-Behnke RG, Liang YX, Tay DKC, Kau PWF, Schneider GE, Zhang S, et al. Nano hemostat solution: immediate hemostasis at the nanoscale. *Nano-medicine* 2006;2:207–15.
- [24] Guo J, Su H, Zeng Y, Liang YX, Wong WM, Ellis-Behnke RG, et al. Reknitting the injured spinal cord by self-assembling peptide nanofiber scaffold. *Nano-medicine* 2007;3:311–21.
- [25] Dégano IR, Quintana L, Vilalta M, Horna D, Borrós S, et al. The effect of self-assembling peptide nanofiber scaffolds on mouse embryonic fibroblast implantation and proliferation. *Biomaterials* 2009;30:1156–65.
- [26] Zhao Y, Yokoi H, Tanaka M, Kinoshita T, Tan T. Self-assembled pH-responsive hydrogels composed of the RATEA16 peptide. *Biomacromolecules* 2008;9: 1511–8.
- [27] Suenaga M. Facio: new computational chemistry environment for PC GAMESS. *J Comput Chem Jpn* 2005;4:25–32.
- [28] Ponder JW, Richards FM. An efficient Newton-like method for molecular mechanics energy minimization of large molecules. *J Comput Chem* 1987;8: 1016–24.
- [29] Guex N, Peitsch MC. SWISS-MODEL and the Swiss-PdbViewer: an environment for comparative protein modeling. *Electrophoresis* 1997;18:2714–23.
- [30] Caplan MR, Schwartzfarb EM, Zhang S, Kamm RD, Lauffenburger DA. Control of self-assembling oligopeptide matrix formation through systematic variation of amino acid sequence. *Biomaterials* 2002;23:219–27.
- [31] Nagayasu A, Yokoi H, Minaguchi JA, Hosaka YZ, Ueda H, Takehana K. Efficacy of self-assembled hydrogels composed of positively or negatively charged peptides as scaffolds for cell culture. *J Biomater Appl*. doi:10.1177/0885328210379927. Available from URL: <http://jba.sagepub.com/content/early/2010/10/29/0885328210379927.abstract>; 2010.
- [32] Friess W. Collagen – biomaterial for drug delivery. *Eur J Pharm Biopharm* 1998;45:113–36.
- [33] Schneider JP, Pochan DJ, Ozbas B, Rajagopal K, Pakstis L, Kretsinger J. Responsive hydrogels from the intramolecular folding and self-assembly of a designed peptide. *J Am Chem Soc* 2002;124:15030–7.
- [34] Schneider GB, English A, Abraham M, Zaharias R, Stanford C, Keller J. The effect of hydrogel charge density on cell attachment. *Biomaterials* 2004;25:3023–8.
- [35] Hattori S, Andrade JD, Hibbs Jr JB, Gregonis DE, King RN. Fibroblast cell proliferation on charged hydroxyethyl methacrylate copolymers. *J Colloid Interface Sci* 1985;104:72–8.
- [36] Seo JH, Matsuno R, Takai M, Ishihara K. Cell adhesion on phase-separated surface of block copolymer composed of poly(2-methacryloyloxyethyl phosphorylcholine) and poly(dimethylsiloxane). *Biomaterials* 2009;30:5330–40.
- [37] Gelain F, Bottai D, Vescovi A, Zhang S. Designer self-assembling peptide nanofiber scaffolds for adult mouse neural stem cell 3-dimensional cultures. *PLoS One* 2006;1(e119):1–11.
- [38] Horii A, Wang X, Gelain F, Zhang S. Biological designer self-assembling peptide nanofiber scaffolds significantly enhance osteoblast proliferation, differentiation and 3-D migration. *PLoS One* 2007;2(e190):1–9.
- [39] Rauch C, Loughna PT. Stretch-induced activation of ERK in myocytes is p38 and calcineurin-dependent. *Cell Biochem Funct* 2008;26:866–9.
- [40] Zhan M, Jin B, Chen SE, Reecy JM, Li YP. TACE release of TNF- α mediates mechanotransduction-induced activation of p38 MAPK and myogenesis. *J Cell Sci* 2007;120:692–701.
- [41] Laboureau J, Dubertret L, Lebretton-De Coster C, Coulomb B. ERK activation by mechanical strain is regulated by the small G proteins rac-1 and rhoA. *Exp Dermatol* 2004;13:70–7.
- [42] Yamaki K, Harada I, Goto M, Cho CS, Akaike T. Regulation of cellular morphology using temperature-responsive hydrogel for integrin-mediated mechanical force stimulation. *Biomaterials* 2009;30:1421–7.
- [43] Wang JG, Miyazu M, Matsushita E, Sokabe M, Naruse K. Uniaxial cyclic stretch induces focal adhesion kinase (FAK) tyrosine phosphorylation followed by mitogen-activated protein kinase (MAPK) activation. *Biochem Biophys Res Commun* 2001;288:356–61.
- [44] Kippenberger S, Bernd A, Loitsch S, Guschel M, Müller J, Bereiter-Hahn J, et al. Signaling of mechanical stretch in human keratinocytes via MAP kinases. *J Invest Dermatol* 2000;114:408–12.
- [45] Boppard MD, Hirshman MF, Sakamoto K, Fielding RA, Goodyear IJ. Static stretch increases c-Jun NH₂-terminal kinase activity and p38 phosphorylation in rat skeletal muscle. *Am J Physiol Cell Physiol* 2001;280:C352–8.